A straightforward access to functionalizable polymers through ring-opening metathesis polymerization of levoglucosenone-derived monomers

Sami Fadlallah, Aurélien A.M. Peru, Amandine Flourat, Florent Allais

A Straightforward Access to Post-Functionalizable Polymers through Ring-Opening Metathesis Polymerization of Levoglucosenone-Derived Monomers

Sami Fadlallah, Aurélien A. M. Peru, Amandine L. Flourat, and Florent Allais**

URD Agro-Biotechnologies Industrielles (ABI), CEBB, AgroParisTech, 51110, Pomacle, France

KEYWORDS: Cellulose-Derived levoglucosenone, HBO, ROMP, Bio-based Polymers, Stereochemical Polymers, Post-Polymerization Modification

ABSTRACT: Levoglucosenone (LGO) is a cellulose-derived and commercially available platform molecule that is produced at an industrial scale. LGO contains a highly reactive double bond that was used to produce two isomers of norbornene-containing LGO monomers, *endo*-N-LGO (**1**) and *exo*-N-LGO (**2**). Furthermore, Baeyer-Villiger oxidation of **1** was performed to yield a highly-valuable chiral monomer, *endo*-N-HBO (**3**). The norbornene moiety of the prepared monomers was readily polymerized by ring-opening metathesis polymerization (ROMP) in the presence of GI catalyst to access highly thermostable polymers with $T_{d5\%}$ up to 360 °C in the case of N-LGO-based polymers and $T_{d5\%}$ in the range of 374-380 °C when **3** was polymerized, such range of $T_{d5\%}$ being the highest reported up-to-date for the LGO-derived polymers. The effect of monomer concentration over the polymerization process was studied and showed that 4 M solutions lead to a better monomer conversion while preserving the control over the polymer structure and reducing the environmental factor (*E* factor). GI was found active in

the ROMP of **3** without the need of protecting the hydroxy group and thus leading to pendent hydroxy functional polymers. Furthermore, for the first time, copolymers containing both LGO and HBO reactive moieties were prepared by random copolymerization of **1** and **3**.

INTRODUCTION

Functional polymers constitute a class of materials carrying valuable features and functionalities, which offers greater reactivity compared to a classical hydrocarbon polymer chain.[1,2] The presence of functional groups, such as carboxylate or hydroxy moieties, not only modulates the chemical, mechanical and thermal properties, but also can efficiently increase the hydrophilicity and degradability of the parent polymers.[3,4] Besides their unique properties, the presence of pendent and/or terminal functional groups on such polymers widen their applications as building blocks and intermediate materials to design new complex structures.[5] Nevertheless, the controlled synthesis of polymers with pendent functionalities is difficult to achieve by direct (co-)polymerization of the related functional monomers due to potential side reactions and lower reactivity/inhibition of the polymerization process.[6] Controlled radical[7] and ionic[8] polymerization techniques were developed and used to enlarge the choice of the monomers, however, several classes of polymers could not be obtained using the mentioned approaches. In this context, diverse methods including ring-opening metathesis polymerization (ROMP) have been studied.[9] ROMP converts cyclic olefins into a wide range of linear polymers with particular architectures and profitable functions.[10,11] For instance, telechelic hydroxy end-functionalized poly(butadiene)s were produced by the ROMP of cyclooctadiene using $(PCy_3)_2Cl_2Ru$=CHPh (Cy = cyclohexyl), known as Grubbs' first-generation catalyst (GI), and an appropriate chain transfer agent (CTA).[12,13] Strained cyclic olefins such as substituted

norbornene derivatives could be used as ROMP monomers,[14] however, the success of the polymerization process depends mostly on the catalyst stability/activity towards these monomers and normally requires the protection of the present functional groups, such as hydroxy, to prevent the deactivation of the catalytic species.[12,14] Moreover, the neighboring functional groups could deactivate the metathesis catalyst unless more than one methylene spacer is present in the monomer.[15] Thus, particular approaches are required to synthesize functional polymers bearing hydroxy group(s) by developing more tolerant metathesis catalysts or/and new functional monomers for well-controlled ROMP.

Biomass is nowadays widely accepted as an eco-friendly, redundant and renewable resource to produce sustainable monomers and polymers carrying different and interesting functionalities.[16–18] In this context, Levoglucosenone (LGO), a versatile α,β-unsaturated cyclic ketone[19,20] derived from cellulosic feedstock[21] (Scheme 1), arose as a promising platform molecule in the preparation of bio-based polymers which can compete with the current fossil-fuel-based commodity polymers. Schlaad and coworkers showed recently that LGO can be used as a readily accessible biomass-derived monomer for the synthesis of thermoplastic polyacetals by ROMP[22] and cationic ring-opening polymerization (CROP).[23]

In the 1980s, Shafizadeh *et al.* and Horton *et al.* reported that the conjugated double bond of the LGO can undergo Diels-Alder cycloaddition with cyclopentadiene (Cp) to produce functionalized carbocycles holding strained norbornene adduct (N-LGO) (Scheme 1).[24,25] Previous studies revealed the behavior of the N-LGO in the oxidation[25,26] and reduction[25,27–29] reactions, for instance, to produce N-HBO and N-(HO)LGO, respectively (Scheme 1), where HBO ((*S*)-γ-hydroxymethyl-α,β-butenolide)[30] is a valuable chiral molecule, readily obtained from LGO using Baeyer-Villiger oxidation, that could be used to

produce valuable compounds[30] such as chiral epoxide.[31] Although LGO is polymerizable on its own by ROMP,[22] Banwell and coworkers demonstrated that having a reactive norbornene moiety on the LGO is of a great interest[32]. Indeed, LGO moieties along the whole backbone chain not only modify the thermal properties of the corresponding polymer, but they also can be used for post-functionalization and thus lead to new polymer architectures with novel properties.

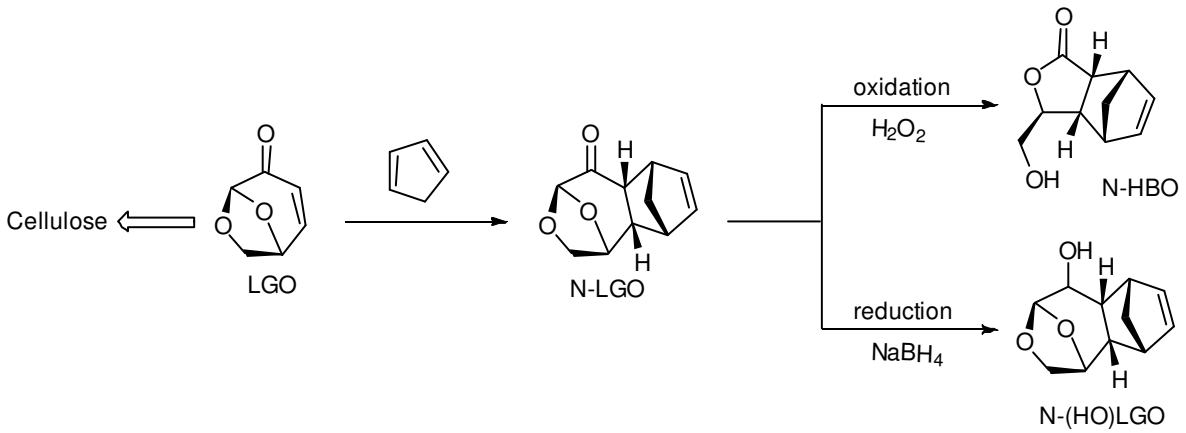

Scheme 1. Synthesis of N-LGO, N-HBO and N-(HO)LGO from LGO

In the present work, we report a new ROMP-based strategy to incorporate cyclic lactones bearing pendent free hydroxy group into the backbone of the polymers through the straightforward homopolymerization and copolymerization of N-LGO and N-HBO monomers, or using post-polymerization modification (*i.e.*, Baeyer-Villiger oxidation) of N-LGO-based polymers (Scheme 2).

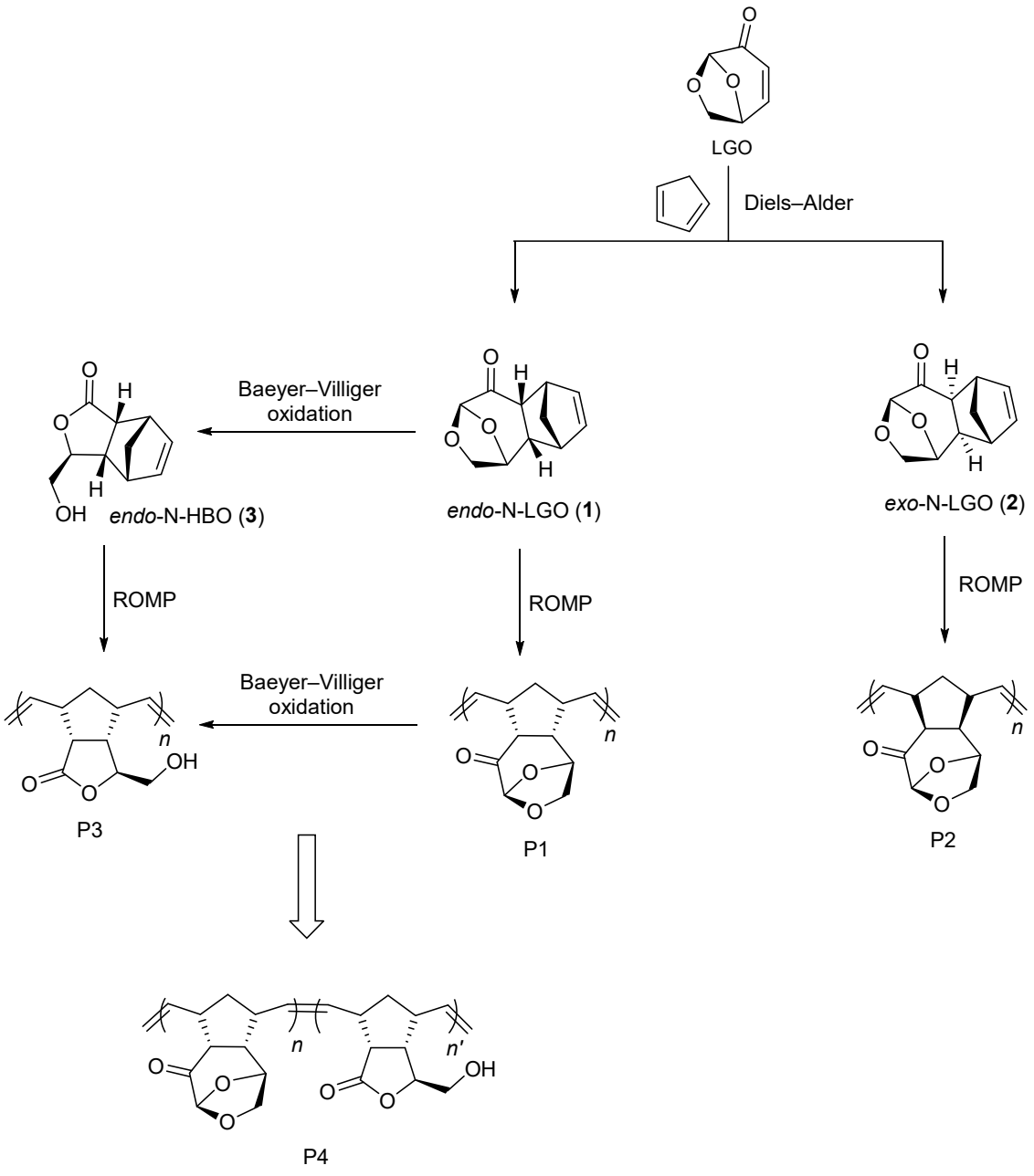

Scheme 2. Synthesis of diverse functional polymers (P1, P2, P3 and P4) from LGO

EXPERIMENTAL SECTION

Chemical and reagents. Levoglucosenone was graciously provided by the Circa group. Aqueous hydrogen peroxide 30% (Fischer), dicyclopentadiene (TCI), Grubbs' 1st generation

catalyst (GI), ethyl vinyl ether, *meta*-chloroperoxybenzoic acid, sodium sulfite, dimethyl sulfide and anhydrous magnesium sulfate were purchased from Sigma Aldrich. The NMR solvents were purchased from Cambridge Isotopes Laboratories. All chemicals and reagents were used as received without purification unless mentioned.

Characterization. *Nuclear Magnetic Resonance (NMR) spectroscopy.* ^{1}H NMR spectra were recorded on a Bruker Fourier 300 MHz ($CDCl_3$ and DMSO-d_6 residual signal at 7.26 and 2.50 ppm respectively). ^{13}C NMR spectra were recorded at 75 MHz ($CDCl_3$ and DMSO-d_6 residual signal at 77.16 and 39.52 ppm, respectively). Chemical shifts are given in parts per million (ppm).

Gas chromatography–mass spectrometry (GC–MS) was performed to study the purity of the monomers using an AgilentGC 5975 coupled with MS 7890 in electron impact mode with electron energy set at 70 eV and a mass range atm/z (30–350 amu). A HP5-MS capillary column (Agilent, 30 m × 0.25 mm, 0.25 μm) was used for chromatographic separation. Injection was performed at 280 °C in split mode (10:1), being injected 1 μL of each sample. The oven temperature program was the following: from 35 °C held for 2 min, then raised until 300 °C at 20 °C/min with a 5 min hold. Hydrogen flow rate was set at 1.2 mL/min. The mass detector was set as follows: source and quad temperatures at 230 and 150 °C, respectively.

Size exclusion chromatography (SEC) was performed at 60 °C using an Agilent Technologies 1260 Infinity Series liquid chromatography system with an internal differential refractive index detector, a viscometer detector, a laser, UV lamp and two PLgel columns (5 μm MIXED-D 300 x 7.5 mm) using 10 mM Lithium Bromide in HPLC grade dimethylformamide as the mobile phase at a flow rate of 1.0 mL/min. Calibration was performed with poly(methyl methacrylate)

Standards. The samples were prepared by solubilizing ~3 mg of material in 1 mL of DMF (10mM LiBr).

Differential Scanning Calorimetry (DSC) thermograms were obtained with a DSC Q20 (TA Instruments). Typically, ~5 mg sample was placed in a sealed pan and was flushed with highly pure nitrogen gas. Various experiments with different heating rates of 10, 20, 30, 40 and 50 °C/ min have been performed in a trial to find the T_g. In addition, various temperature ranges were applied from -80 °C to 100, 120, 140, 160, 200 and 300 °C.

Thermogravimetric Analysis (TGA) was measured with a TGA Q500 (TA Instruments). Typically, ~1 mg of each sample was equilibrated at 50 °C for 30 min and was flushed with highly pure nitrogen gas. All the experiments were performed with a heating rate of 10 °C/min up to 600 °C. The reported values $T_{d5\%}$ and $T_{d50\%}$ represent the temperature at which 5% and 50% of the mass is lost, respectively.

Synthesis of Monomers. *Diels alder reaction of LGO and cyclopentadiene.* Dicyclopentadiene (100 mL, 742 mmol, 2.8 equiv.) was distilled under atmospheric pressure at 180 °C to form cyclopentadiene which was added directly to a solution of levoglucosenone (33 g, 262 mmol) in dichloromethane at room temperature. The reaction mixture was stirred at room temperature during 40 h and concentrated to dryness. The residue was purified by silica chromatography (gradient: 95/5 to 70/30 cyclohexane/Ethyl acetate as eluent) to give 32 g of *endo*-product (**1**) (64%, white solid) and 0.5 g of *exo*-product (**2**) (1%, oil) (and 4.3 g, 13%, of unreacted levoglucosenone). Analytical data matched those reported by Shafizadeh *et al.* and Horton *et al.*[24,25]

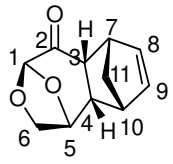

^{1}H NMR ($CDCl_3$) δ (ppm): 6.23 (dd, *J* = 3.0 and 5.4 Hz, 1H, H_9), 6.02 (dd, *J* = 2.7 and 5.7 Hz, 1H, H_8), 4.81 (s, 1H, H_1), 4.63 (d, *J* = 4.5 Hz, 1H, H_5), 3.83 (tapp, *J* = 6.0 Hz, 1H, H_{6a}), 3.77 (tapp, *J* = 4.8 Hz, 1H, H_{6s}), 3.38 (br.s, 1H, $H_{7,}$), 3.02 (m, 1H, H_{10}), 2.99 (m, 1H, H_3), 2.39 (dd, *J* = 3.6 and 9.3 Hz, 1H, H_4), 1.46 (dt, *J* = 1.8 and 6.6 Hz, 1H, H_{11s}), 1.30 (dt, *J* = 2.0 and 8.4 Hz, 1H, H_{11a}).

^{13}C NMR ($CDCl_3$) δ (ppm): 200.4 (C_2), 135.6 (C_8 and C_9), 134.30 (C_1), 99.3 (C_5), 74.9 (C_6), 70.3 (C_4), 49.5 (C_{11}), 46.9 (C_7), 46.4 (C_3), 42.4 (C_{10}).

Baeyer-Villiger oxidation of endo-N-LGO. A 30% aq. hydrogen peroxide solution (50 mL, 500 mmol, 5 equiv.) was added dropwise to a stirred solution of *endo*-N-LGO (**1**) (19 g, 100 mmol) in isopropanol (250 mL) and 80% phosphoric acid (8 mL, 1.2 equiv.). The reaction mixture was stirred at 80 °C for 1 day. To the cooled reaction was added an aqueous solution of sodium sulfite till the consumption of the excess oxidizing species. The reaction mixture was then concentrated and extracted with ethyl acetate. The organic layer was washed with brine, dried over anhydrous magnesium sulfate and evaporated to dryness. The crude product was purified by silica gel chromatography (gradient: 90/10 to 20/80 cyclohexane/Ethyl acetate as eluent) to give 10.6 g of *end*o-N-HBO (**3**) (59%, white solid). Analytical data matched those reported by Davydova and coworkers.[28]

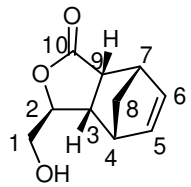

^{1}H NMR ($CDCl_3$) δ (ppm): 6.28 (dd, J = X and Y Hz, 1H, H_6), 6.26 (dd, *J* = 2.7 and 5.7 Hz, 1H, H_5), 4.02 (dt, *J* = 1.5 and 3.2 Hz, 1H, H_2), 3.80 (dd, *J* = 3.0 and 12.3 Hz, 1H, H_{1s}), 3.62 (dd, *J* = 4.5 and 12.3 Hz, 1H, H_{1a}), 3.31 (m, 1H, H_7), 3.27 (m, 1H, H_9), 3.12 (m, 1H, H_4), 2.93 (m, 1H,

H_3), 3.14 (br.s, 1H, OH), 1.64 (dt, *J* = 1.2 and 8.4 Hz, 1H, H_{8s}), 1.45 (dt, *J* = 1.2 and 8.4 Hz, 1H, H_{8a}).

^{13}C NMR ($CDCl_3$) δ (ppm): 178.2 (C_{10}), 136.7 (C_5), 134.7 (C_6), 82.9 (C_2), 64.8 (C_1), 51.7 (C_3), 48.7 (C_8), 45.8 (C_7), 45.5 (C_9), 42.7 (C_4).

Polymerizations. *ROMP of endo-N-LGO. endo*-N-LGO and GI were weighed and mixed in a Schlenk flask followed by three purges of vacuum/nitrogen. Anhydrous dichloromethane was added to the mixture and the reaction was stirred at room temperature for a predetermined time. An aliquot of the obtained solution was taken and evaporated to dryness to determine the extent of conversion by ^1H NMR in $CDCl_3$. At the end of the reaction, the medium was viscous, the polymerization was quenched by adding ethyl vinyl ether in dichloromethane. The solution was precipitated from methanol two times to remove the catalyst, ethyl vinyl ether and unreacted monomers. The formed solid polymer, P1, was vacuum dried overnight.

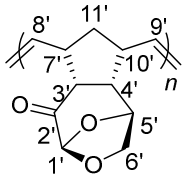

^1H NMR ($CDCl_3$) δ (ppm): 5.74 (m, 1H, $H_{9'}$), 5.62 (m, 1H, $H_{8'}$), 4.93 (s, 1H, $H_{1'}$), 4.74 (m, 1H, $H_{5'}$), 3.84 (m, 1H, $H_{6'a}$), 3.78 (m, 1H, $H_{6's}$), 3.05 (m, 1H, $H_{7'}$), 2.82 (m, 2H, $H_{3'}$ and H_{10}'), 2.47 (m, 1H, $H_{4'}$), 1.92 (m, 1H, $H_{11's}$), 1.62 (m, 1H, $H_{11'a}$).

^{13}C NMR ($CDCl_3$) δ (ppm): 203.6 ($C_{2'}$), 132.6 ($C_{8'}$), 130.8 ($C_{9'}$), 100.1 ($C_{1'}$), 73.6 ($C_{5'}$), 69.2 ($C_{6'}$), 50.2 ($C_{7'}$), 49.6 ($C_{10'}$), 47.3 ($C_{3'}$), 46.1-45.2 ($C_{11'}$), 41.4-38.3 ($C_{4'}$).

ROMP of exo-N-LGO. exo-N-LGO and GI were weighed and charged in two separate Schleck flasks followed by three purges of vacuum/nitrogen. Anhydrous dichloromethane was added to

GI then the prepared catalyst solution was transferred over the syrup *exo*-adduct. After, the reaction proceeded following a similar procedure as for P1 to afford P2.

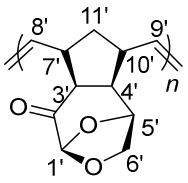

^{1}H NMR ($CDCl_3$) δ (ppm): 5.56 (m, 1H, $H_{9'}$), 5.36 (m, 1H, $H_{8'}$), 5.12 (m, 1H, $H_{1'}$), 4.54 (m, 2H, $H_{5'}$), 3.93 (m, 1H, $H_{6'a}$), 3.85 (m, 1H, $H_{6's}$), 3.30 (m, 1H, $H_{7'}$), 2.94 (m, 2H, $H_{3'}$), 2.71 (m, 1H, H_{10}'), 2.45 (m, 1H, $H_{4'}$), 2.03 (m, 1H, $H_{11's}$), 1.25 (m, 1H, $H_{11'a}$).

ROMP of endo-N-HBO. The reaction proceeded following a similar procedure as for the ROMP of *endo*-N-LGO. However, at the end of the reaction, the polymers were insoluble in dichloromethane. Thus, the polymerization was quenched by adding ethyl vinyl ether in dimethylformamide. Then precipitated from methanol to afford P3.

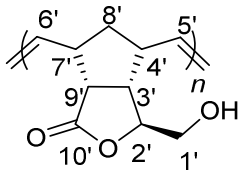

^{1}H NMR (DMSO-d_6) δ (ppm): 5.57 (m, 1H, $H_{6'}$), 5.43 (m, 1H, $H_{5'}$), 5.03 (m, 1H, OH), 4.29 (m, 1H, $H_{2'}$), 3.53 (m, 2H, $H_{1's,a}$), 3.17 (m, 1H, $H_{7'}$), 3.06-2.78 (m, 1H, $H_{9'}$, $H_{4'}$ and $H_{3'}$), 1.76 (m, 1H, $H_{8's}$), 1.34 (d, 1H, $H_{8'a}$).

^{13}C NMR (DMSO-d_6) δ (ppm): 176.6 ($C_{10'}$), 131.1 ($C_{5'}$), 128.7 ($C_{6'}$), 80.5 ($C_{2'}$), 63.1 ($C_{1'}$), 48.5 ($C_{9'}$), 45.0 ($C_{4'}$), 44.2 ($C_{7'}$), 38.0-37.5 ($C_{8'}$), 35.5 ($C_{3'}$).

Random Copolymerization. *endo*-N-LGO, *endo*-N-HBO and GI were weighed and mixed in a Schlenk flask followed by three purges of vacuum/nitrogen. Anhydrous dichloromethane was

added to the mixture and the reaction was stirred at room temperature for a predetermined time. An aliquot of the obtained solution was taken and evaporated to dryness to determine the extent of conversion by ^{1}H NMR measurements in $CDCl_3$. At the end of the reaction, the polymerization was quenched by adding ethyl vinyl ether in dimethylformamide. The solution was precipitated from methanol 2 times to remove the catalyst, ethyl vinyl ether and unreacted monomers.

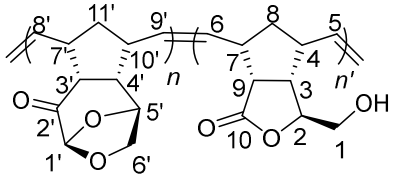

^{1}H NMR (DMSO-d_6) δ (ppm): 5.71-5.41 (m, 4H, H_5, H_6, $H_{8'}$ and $H_{9'}$), 5.00 (m, 1H, OH), 4.93(m, 2H, $H_{1'}$), 4.67 (m, 1H, $H_{5'}$), 4.23 (m, 1H, H_2), 3.74 (m, 1H, $H_{6'}$), 3.54 (m, 2H, H_1), 3.09-2.72 (m, 8H, H_3, H_4, H_7, H_9, $H_{3'}$, $H_{4'}$, $H_{7'}$ and $H_{10'}$), 1.79 (br.s, 2H, H_{8s} and $H_{11's}$), 1.44 (br.s, 2H, H_{8a} and $H_{11'a}$).

^{13}C NMR (DMSO-d_6) δ (ppm): 204.4 ($C_{2'}$), 176.7 (C_{10}), 132.0-128.5 (C_5, C_6, $C_{8'}$, $C_{9'}$), 98.9 ($C_{1'}$), 98.5 ($C_{5'}$), 72.8 (C_2), 68.3 ($C_{6'}$), 63.0 (C_1), 49.4 ($C_{7'}$), 49.0 ($C_{3'}$), 45.9 (C_4), 45.4 (C_7), 44.7 (C_8), 44.1 (C_9), 38.1 ($C_{10'}$), 35.8 ($C_{4'}$), 30.7 (C_3).

Baeyer-Villiger Oxidation of P1. Under N_2, P1 (0.05 g, 0.26 mmol) was dissolved in anhydrous dichloromethane (5 mL). At 0 °C, *m*-CPBA (0.09 g, 0.52 mmol, 2 equiv.) was added. The reaction mixture was stirred at room temperature for 24 h, then quenched by adding Me_2S (39 µL, 0.52 mmol). After 15 min of stirring, the solvent was removed by evaporation under reduced pressure. The crude mixture was dissolved in dimethylformamide (2 mL). The desired product was recovered by precipitation in methanol and filtration.

RESULTS AND DISCUSSION

Preparation and stereoisomerism of the N-LGO and N-HBO monomers. Two isomers of the N-LGO monomer were prepared following the method described by Horton and co-workers[25] with slight modifications including the direct distillation of dicyclopentadiene, to recover pure Cp,[33] into a solution containing LGO. A major crystalline *endo* isomer (*endo*-N-LGO (**1**), 64%) was isolated when the conjugated double bond of LGO was oriented towards the Cp diene system in the transition state, in contrast, the *exo* transition state was attained if it was oriented away to produce a syrupy *exo* isomer (*exo*-N-LGO (**2**), 1%) (Scheme 3). A full and comprehensive analysis of the two products by NMR spectroscopy was reported by Shafizadeh *et al.* and Horton *et al.*[24,25] Starting from *endo*-N-LGO, we envisioned to access enantiopure *endo*-N-HBO (**3**), through Baeyer-Villiger oxidation (BVO). As our in-house organic solvent- and catalyst-free H_2O_2-mediated BVO[34] proved unsuccessful, we thus performed the H_3PO_4-catalyzed and H_2O_2-mediated BVO to access the hydroxy-lactone **3** from the orthoformate intermediate (Schemes 2 and 3). Furthermore, it is noteworthy to mention that a polar solvent such as isopropanol increased the rate of the oxidation reaction.[28]

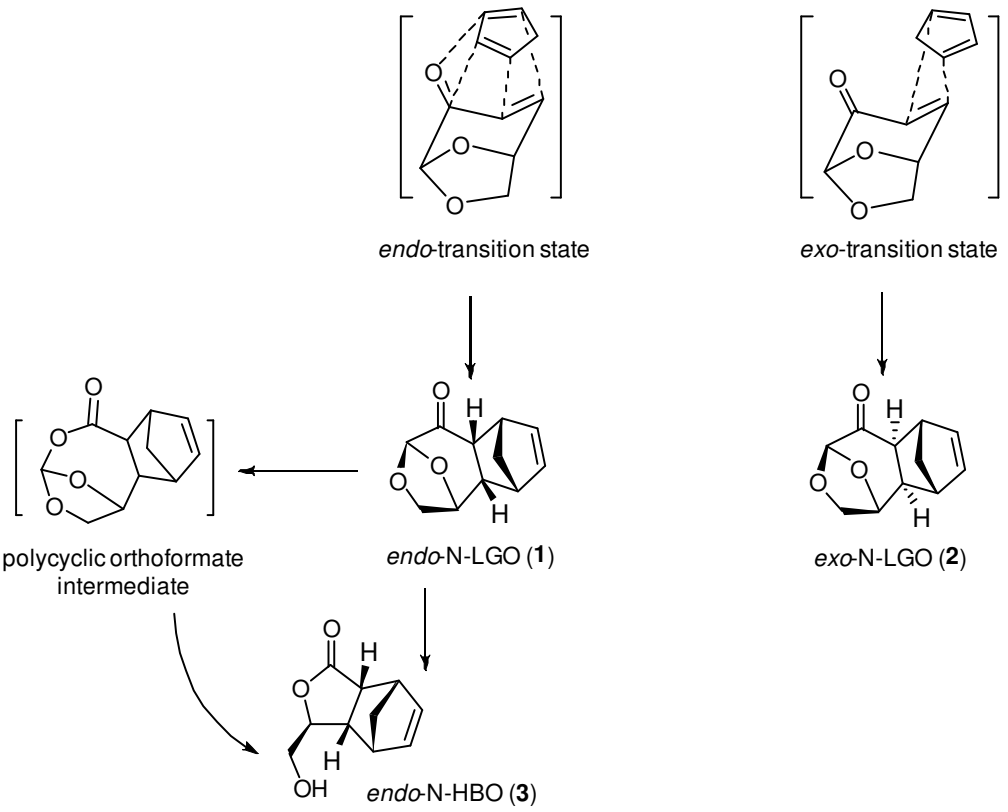

Scheme 3. Synthesis of N-LGO and N-HBO isomers including a schematic representation of the transition states

*Polymerization of **1** and **2***. An easy-to-make and inexpensive Ru catalyst called GI was adopted in this study due to its better functional group tolerance[35],[36] and convenient use (low oxophilicity) compared to other transition metal complexes.[37] Dichloromethane (DCM) was chosen for better solubility of the polymers produced as well as to attain better catalyst efficiency; these ROMPs were conducted at room temperature to avoid undesired rapid catalyst decomposition (Table 1).

Table 1. Polymerization of **1** and **2** using $(PCy_3)_2Cl_2Ru$=CHPh, GI

Entry [a]	[N-LGO] (M) [b]	[N-LGO]/[GI] [c]	t (h)	Conv. (%) [d]	$M_{n(SEC)}$ (kg.mol^{-1}) [e]	$Đ$ [e]	$T_{d5\%}$ [f]	$T_{d50\%}$ [f]
1	2	100	22	98	25.0	1.10	336	489
2	2	100	5	62	27.4	1.13	347	443
3	4	100	5	72	28.4	1.09	344	436
4 [g]	4	100	1	90	31.0	1.16	290	444
5	2	500	22	56	66.6	1.27	337	438
6	4	500	22	67	97.1	1.20	350	435
7	4	500	5	36	56.3	1.08	339	435
8	4	1000	5	31	60.0	1.08	349	439
9	4	1000	22	45	121.9	1.19	360	438

[a] *endo*-N-LGO (**1**) was used as the monomer unless otherwise specified, n(**1**) = 1.04 mmol, dichloromethane was used as solvent, T = 22 °C. [b] N-LGO concentration in M. [c] Ratio given per equivalent of metal atom. [d] Conversion determined by ^{1}H NMR spectroscopy in $CDCl_3$. [e] Determined by SEC in DMF (10 mM LiBr) at 60 °C against poly(methyl methacrylate) standards, $Đ$ = dispersity. [f] TGA degradation temperatures at which 5% ($T_{d5\%}$) and 50% ($T_{d50\%}$) mass loss was observed under nitrogen. [g] *exo*-N-LGO (**2**) was used as the monomer, n(**2**) = 1.04 mmol.

The first series of ROMPs was directed towards **1** (entries 1-3 and 5-9, Table 1) rather than **2** (entry 4, Table 1) due to its high synthetic yield and easy-to-use crystalline form. In contrast to what was recently reported by Banwell and coworkers for the ROMP of N-isoLGO (isoLGO is the pseudo-enantiomer of N-LGO),[32] GI revealed a good activity in the ROMP of **1**. Indeed, 100 equiv. of **1** (2 M in DCM) were polymerized, in the presence of GI (1 equiv.), at an acceptable rate where 62% and 98% of the monomers were converted to afford P1 (as a white solid when precipitated from methanol) in 5 h (entry 2, Table 1) and 22 h (entry 1, Table 1), respectively. Increasing the monomer-to-catalyst ratio ([M]/[C]) to 500 inquired longer duration to combine the monomer units, *e.g.* for a 22 h reaction time, lesser conversion (56%) of **1** was obtained (entry 5, Table 1). The ring-opening of the norbornene adduct was confirmed by ^{1}H

NMR analysis of the polymers (Figure S6 in the Supporting Information) with the appearance of two multiplet resonances at 5.74 ($H_{9'}$) and 5.62 ($H_{8'}$) ppm, accompanied with the complete disappearance of the cyclic alkene at 6.23 (H_9) and 6.02 (H_8) ppm after purification. The separation of the alkene peaks into two sets is due to the carbonyl anisotropy effect, in addition, the two bridged protons of the opened norbornene came out as two separate peaks, $H_{11's}$ (*s* for *syn*) and $H_{11'a}$ (*a* for *anti*) at 1.93 and 1.59 ppm, respectively, due to the anisotropic effect of the double bonds. The *cis* and *trans* contents of P1 was examined by ^{13}C NMR (Figure S10, Supporting Information) and showed the uncontrolled existence of both configurations as reported recently by Banwell and coworkers.[32] The tacticity of N-LGO polymers was likewise elucidated using ^{13}C NMR, and multiple resonances corresponding to an atactic polymer were observed in the region of 46.1-45.2 ($C_{11'}$) . A possible explanation for such behavior is the slow propagation rate of the incorporated monomers with respect to the carbine epimerization. Interestingly, Banwell and coworkers highlighted the good activity of the second- and third-generation Grubbs' catalysts (GII and GIII, respectively), in addition to the second-generation Hoveyda-Grubbs' catalyst (HGII) and the Stewart-Grubbs' catalysts in the ROMP of N-isoLGO.[32] However, the authors chose to conduct the polymerization reactions in DCM diluted solutions, which in turn increases the amount of waste generated and thus increases the environmental factor (*E* factor).[38] We estimated the *E* factor (excluding the work-up solvents to allow the comparison) of an experiment performed at 0.5 M substrate concentration as 13.9 kg of waster/kg of polymer with 93% of solvent contribution to the value (entry 1, Table S1 in the Supporting Information). Keeping the same [M[/[C] ratio (250) while performing the reaction in a more concentrated medium (4 M) will result in a considerable decrease of the *E* factor to 1.7 (entry 2, Table S1 in the Supporting Information), which demonstrates the necessity to reduce

the amount of solvent, especially when dealing with toxic solvents such as DCM, for the sake of potential industrialization of promising polymers such as LGO-derived polymers.

We thus decided, in this work, to increase the concentration of **1** from 2 to 4 M. This resulted in an increase in conversion from 62% to 72% (entries 2 and 3 respectively, Table 1), and from 56% to 67% (entries 5 and 6 respectively, Table 1) while preserving the polymerization control as will be later described in this article. Consequently, we recorded a remarkable decrease in the *E* factor, from 6.0 to 2.8 kg of waster/kg of polymer, if entries 2 (2 M) and 3 (4 M) are respectively applied. The calculations of these two values are shown in Table S1 in the Supporting Information, entries 3 and 4.

Thereupon, we decided to study the effect of stereochemistry on the polymerization rate by applying the *exo*-N-LGO isomer (**2**) under the previously optimized conditions for **1** (entry 4, table 1). As perceived, the ROMP underwent faster, with 90% conversion in less than 1 h to give P2 (Figure S8, Supporting Information). It is likely that in **1** the ketone group of the LGO moiety (located in *syn* position to the alkene bond) slowed down the coordination of the Ru center. In contrast, the ketone group of **2** placed in an *anti*-position and farthest to the olefin and hence a better approach to the catalyst was achieved. Another possible reason for the lower catalyst activity towards **1** is the simultaneous chelation of the metal center with the double bond and the ketone functional group. Moore and coworkers reported a similar behavior for the ROMP of *exo-vs. endo*-dicyclopentadiene.[39]

The SEC chromatograms of all purified polymers (P1 and P2) displayed unimodal profiles (Figures S15 and S16 respectively, in the Supporting Information), in addition, the observed molecular weights ($M_{n(SEC)}$) increased with the increase of [M]/[C] ratio under the same reaction

conditions with narrow dispersity (*Đ*) ranging from 1.08 to 1.27. Furthermore, a high M_W polymer was obtained, $M_{n(SEC)}$ = 121.9 kg.mol^{-1} with *Đ* = 1.19, when a feed ratio of 1000 was applied (entry 9, Table 1). The $M_{n(SEC)}$ of the produced polymers were found higher than the theoretical values ($M_{n(theo)}$), *e.g.* 25.0 kg.mol^{-1} (entry 1, Table 1) *vs.* 18.7 kg.mol^{-1} for the $M_{n(theo)}$. This could be explained by the existence of deactivated/dead catalysts or/and a high propagation rate of the polymers that could exceed the catalyst initiation rate leading to high M_W polymers at the early stage of the polymerization. This is a typical behavior of a non-living character and was already observed for the polyacetals produced from the ROMP of LGO.[22]

We explored the thermal properties of P1 and P2 *via* thermogravimetric analysis (TGA) and differential scanning calorimetry (DSC). The TGA thermograms (*e.g.* Figures S22-S26 in the Supporting Information) show, for some samples, a slight weight loss during the equilibrium stage at 50 °C which corresponds to the solvent removal from the polymers. Very interestingly, the TGA analysis demonstrated that P1 is thermostable up to 360 °C with 5% decomposition ($T_{d5\%}$) and up to 489 °C where 50% of the polymer was degraded ($T_{d50\%}$) (entries 1-3 and entries 5-9, Table 1), such thermal behavior is unprecedented for the LGO-derived polymers and it is far more different from those reported by Banwell and coworkers ($T_{d5\%}$ up to 168 °C) and by Schlaad and coworkers ($T_{d5\%}$ up to 220 °C). The TGA thermogram of P2 displayed a $T_{d5\%}$ at 290 °C (Figure S26 in the Supporting Information), such decrease in T_d could be consistent with more randomness in the atactic structure of P2 compared to P1 which leads to a less rigid structure and in turn a decrease in degradation temperature.

All our attempts to find the T_g of P1 and P2 during the 2nd or 3rd cycle of the DSC analysis failed, (no thermal transitions in the structure were observed). Indeed, heating up to 200 °C during the first cycle induced the polymers crosslinking, encountered by an exothermic transition

at 180-200 °C (Figures S32-34, Supporting Information), most probably due to the presence of reactive acetal functions in the repeating LGO moieties.[40] Besides, various unrepeatable phase transitions were also observed during the first cycle and thus they are not shown or discussed in this work. The crosslinking of the polymers was confirmed by performing a thermal post-treatment of P1 at 200 °C which resulted in polymer insolubility in chloroform, in addition to a change in color from white to brown (Figure S1 in the Supporting Information) accompanied with a texture transformation from soft to brittle (Figures S32-34, Supporting Information, shows the crystalline transition by DSC). We then attempted to change the temperature range of the DSC analysis from -50 to 100, 120, 140 and 160 °C, however no obvious T_g appeared to exist.

Post-polymerization modification of P1. We examined the BVO of P1 (isolated from entry 1, Table 1) following the same conditions applied to oxidize **1** into **3**, however the polymer was recovered intact after the reaction, as the LGO moieties along the polymer backbone resisted the oxidation. Thus, we envisioned a *meta*-chloroperoxybenzoic acid (*m*-CPBA)-mediated BVO (2 equiv. per monomer repeating unit) of a polymer prepared using 30 equiv. of **1** ($M_{n(SEC)}$ = 11.7 kg.mol^{-1}, $Đ$ = 1.24). The color changed from colorless to brownish after a few hours in DCM solution at room temperature accompanied with the formation of precipitate. The reaction was stopped after 24 h by adding Me_2S to quench the excess of *m*-CPBA followed by precipitation in methanol to collect a non-DCM-soluble polymer chain with $M_{n(SEC)}$ = 8.3 kg.mol^{-1}, $Đ$ = 1.47 having likely HBO moieties as confirmed by the solubility and TGA analysis that showed an increase in $T_{d5\%}$ from 323 to 361 °C after the BVO (Figures S27 and S28 respectively in the Supporting Information). A similar behavior was recorded for the N-HBO based polymer as will be discussed in the next section. However, it is important to note that the NMR analysis of the

polymer is not fully consistent with the formation of 100% N-HBO ROMP-analogue as it shows some peaks which may correspond to oxidized olefin moieties.

*Polymerization of **3**.* We sought to study the ROMP of **3** using GI without protecting the hydroxy group of the HBO moiety to not only eliminate solvent-, reagents- and energy-consuming and waste-generating steps such as protection and deprotection which greatly increase the *E* factor of the process, but also to demonstrate further the interest of the studied molecule as a monomer allowing the direct access to hydroxy-functional polymers. Indeed, polarization or coordination effect by neighboring functional group(s) normally lead to the catalyst deactivation unless more than one methylene spacers are present between the olefin and any functionality. In our case, the hydroxy group of **3** is separated by four carbon atoms from the double bond and at the same time, attached into a rigid 5-membered lactone ring, which limit its rotation, and decrease the chance to approach the coordinated Ru catalyst.

The ROMP of **3** was attempted in DCM at room temperature and an interesting different behavior was observed compared to **1** (Table 2). Notably, the polymerization rate was higher when a feed ratio of 100 equiv. of **3** was applied (entry 13, Table 2) to yield 92% of non-DCM-soluble P3 in less than 4h. Notably, the same color and behavior was recorded for P3 as for the polymer obtained after the BVO of P1. The difference in reactivity of **1** and **3** can be explained by a lower anisotropy effect of C=O with respect to the *endo* double bond (in the case of **3**) and this could lead to a better approach of the catalyst to the olefin and weaker coordination between the Ru center and the carbonyl group. Nevertheless, a significant drop in conversion was clearly observed when we increased the [M]/[C] ratio to 500 equiv. (entries 11 and 12 compared to entry 10, Table 2) and 1000 equiv. (entries 14 and 15 compared to entry 13, Table 2) and this is due to the significant increase in the number of hydroxy monomers which can deactivate/decompose

the catalyst as discussed previously in the introduction. ^{1}H NMR in DMSO-d_6 (Figure S7 in the Supporting Information) showed the opening of the norbornene ring at 5.59- 5.43 ppm ($H_{6'}$ and $H_{5'}$) and no traces of unreacted olefin appeared to exist at 6.28 (H_6) and 6.15 (H_5) ppm after precipitation from methanol. Furthermore, the hydroxy group appearing at 5.03 ppm is a proof of the pendent functional group along the backbone chain. Again, and due to the anisotropic effect of the double bonds, the bridged protons at position 8 generate two different peaks at 1.76 ($H_{8's}$) and 1.35 ($H_{8'a}$) ppm.

As in the case of **1** and **2**, the SEC analysis showed unimodal curves for entries 10-15 (*e.g.* Figure S17 in the Supporting Information) and $M_{n(SEC)}$ was dependent on the [M]/[C] and monomer conversion. An increase of $M_{n(SEC)}$ was recorded at higher feed ratios, *e.g.* 28.1 kg.mol^{-1} when the reaction tube was charged with 500 equiv. of **3** (entry 14, Table 2) *vs.* 76.7 kg.mol^{-1} in the case of 1000 equiv. (entry 15, Table 2). Again, a mismatch of $M_{n(SEC)}$ and $M_{n(theo)}$ occurred for the same reason as discussed previously. Moreover, in diluted condition (2 M) P3 displayed better dispersity of the chains ($Đ$ = 1.21 and 1.20 for entries 11 and 12, respectively, Table 2) compared to 4 M solutions ($Đ$ = 1.58 and 1.56 for entries 11 and 12, respectively, Table 2)

Table 2. Polymerization of **3** using $(PCy_3)_2Cl_2Ru$=CHPh, GI

Entry [a]	**[3]** [b]	**[3]/[GI]** [c]	***t*** **(h)**	**Conv. (%)** [d]	$M_{n(SEC)}$ **(kg.mol^{-1})** [e]	$Đ$ [e]	$T_{d5\%}$ [f]	$T_{d50\%}$ [f]
10	2	100	22	71	57.9	1.22	377	449
11	2	500	22	23	54.7	1.21	374	447
12	2	1000	22	17	32.7	1.20	379	446
13	4	100	4	92	44.2	1.17	378	448
14	4	500	22	12	28.1	1.58	370	447
15	4	1000	22	19	76.7	1.56	380	447

[a] n(**3**) = 1.11 mmol, dichloromethane was used as solvent, T = 22 °C. [b] Concentration of **3** in M. [c] Ratio given per equivalent of metal atom. [d] Determined by ^{1}H NMR spectroscopy in DMSO-d_6. [e] Conversion determined by SEC in

DMF (10 mM LiBr) at 60 °C against poly(methyl methacrylate) standards, $Đ$ = dispersity. [f] TGA degradation temperatures at which 5% ($T_{d5\%}$) and 50% ($T_{d50\%}$) mass loss was observed under nitrogen.

Notably, the TGA analysis demonstrated that P3 are more thermally stable than P1 and P2 with $T_{d5\%}$ ~ 380 °C and $T_{d50\%}$ ~ 449 °C (entries 10-15, Table 2) (Figures S29-S31 in the Supporting Information) which makes them the most thermostable LGO-derived polymers up-to-date.[22,23,32,41–44] The analysis of P3 by DSC showed the same behavior as P1 and P2 (Figure S35, Supporting Information) and no T_g value clearly appeared during the 2nd or 3rd cycle of the analysis. It is important to note that some changes were observed, however they were not reproducible and thus they are not shown herein.

*Copolymerization of **1** and **3**.* Looking at the interesting properties of the polymers P1 and P3, we then focused on the statistical copolymerization of **1** and **3**, under mild conditions, in 2 M DCM solutions at room temperature, in the presence of GI (Table 3). The [*endo*-N-LGO]/[*endo*-N-HBO] ([**1**]/[**3**]) ratio was varied to study the impact of each monomer on the copolymers obtained and on the conversion and percentage of incorporation. The difference in the chemical shifts of the homo-dyads ((**1**-**1**) and (**3**-**3**)) and hetero-dyads ((**1**-**3**) and (**3**-**1**)) was not detectable by NMR spectroscopy (Figures S9 and S12, Supporting Information), however, as expected, a better conversion of **1** was achieved whatever the [**1**]/[**3**] ratio (entries 16-18, Table 3), *e.g.* 91% of **1** and 35% of **3** were converted when equimolar ratio of the two monomers was applied (entry 16, Table 3). This is consistent with the results obtained in 2 M solutions for the homopolymerization of **1** or **3** (Tables 1 and 2, respectively). Nevertheless, an increase of N-HBO units in the copolymer's chain was observed at higher feed ratio of **3**, where 29% of the latter was incorporated if we doubled the initial quantity of **3** with respect to **1** (entry 18, Table 3). This percentage dropped to 16% at equimolar ratio (1/1) (entry 16, Table 3) and to 9% for 2/1

equivalents of **1** *vs.* **3** (entry 17, Table 3). Such controlled incorporation of monomer **3** provides insights into the control over the copolymerization reactions which can be also highlighted by the unimodal SEC traces of the copolymers where no homopolymers appeared to exist (Figures S19-S21 in the Supporting Information). Furthermore, relatively narrow *Đ* values were registered (*Đ* = 1.42, 1.39 and 1.49 for entries 16, 17 and 18 respectively, Table 3). Unfortunately, the T_g values were out of reach through DSC analysis (due to the same reasons described previously) and thus we were not able to compare the effect of the percentage of incorporation of both monomers on the thermal properties of the copolymers. As expected TGA analysis showed that the copolymers prepared are quite stable with $T_{d5\%}$ up to 331 °C (entry 16, Table 3).

Table 3. Copolymerization of **1** and **3** using $(PCy_3)_2Cl_2Ru$=CHPh, GI

Entry [a]	**[1]/[3]**	**Conv. (%)** [b]		**Comp. (%)** [c]		$M_{n(SEC)}$ **(kg.mol^{-1})** [d]	*Đ* [d]	$T_{d5\%}$ [e]	$T_{d50\%}$ [e]
		N-LGO	N-HBO	N-LGO	N-HBO				
16	1/1	91	35	84	16	35.9	1.42	331	456
17	2/1	88	21	91	9	35.2	1.39	316	436
18	1/2	85	24	71	29	25.9	1.49	310	465

[a] [**1** + **3**]/[GI] = 100, for equimolar ratio of monomers n(**1**) = n(**3**) = 0.52 mmol, dichloromethane was used as solvent, concentration equal to 2 M, T = 22 °C, t = 22 h. [b] Conversion of the monomers determined by ^{1}H NMR spectroscopy of an aliquot of the reaction mixture in DMSO-d_6. [c] Percentages of N-LGO and N-HBO units in the copolymer determined by ^{1}H NMR spectroscopy of an isolated copolymer in DMSO-d_6. [d] Determined by SEC in DMF (10 mM LiBr) at 60 °C against poly(methyl methacrylate) standards, *Đ* = dispersity. [e] TGA degradation temperatures at which 5% ($T_{d5\%}$) and 50% ($T_{d50\%}$) mass loss was observed under nitrogen.

CONCLUSION

Commercially available at the ton/year scale, LGO was used as a sustainable starting material to produce two partially bio-based LGO-derived monomers, *endo*-N-LGO (**1**) and *exo*-N-LGO (**2**). Furthermore, **1** was successfully subjected to BVO to afford a highly-valuable chiral monomer, *endo*-N-HBO (**3**). As we are dealing with potential industrial-scale polymers, concentrated ROMPs were performed to pave the way toward more environmentally friendly reactions by

decreasing the *E* factor from 6.0 to 2.8 kg of waster/kg of P1. The effect of the stereochemistry of N-LGO monomers on the polymerization was examined and showed that the ROMP proceeds faster with the *exo*-isomer **2**. The ROMP of **3** was successfully performed without the need to protect the hydroxy group of HBO, the interest of such approach relies on *i*) the decrease of the overall *E* factor of the process by avoiding the protection and deprotection steps, and *ii*) the direct access to free hydroxy-pendent functional polymers from simply prepared monomers such as **3**. Copolymers of **1** and **3** were synthesized by the random copolymerization of these monomers under mild conditions. The incorporated portion of monomer **3** was controlled by the ratio of [**1**]/[**3**] where a composition of 29% of N-HBO units was recorded at a doubled feed ratio of **3** with respect to **1**. SEC chromatograms displayed unimodal profiles for all polymers produced in this study, along with narrow *Đ*. Very interestingly, the TGA analysis demonstrated that the polymers are quite thermally stable, with $T_{d5\%}$ up to 360 °C and $T_{d50\%}$ up to 489 °C for P1, and $T_{d5\%}$ ~380 °C and $T_{d50\%}$ ~449 °C for P3, such thermal behavior is unprecedented for the LGO-derived polymers. These polymers constitute a useful addition to the recent evolving family of LGO-derived polymers and can be employed as building blocks – thanks to the presence of LGO or/and HBO reactive moieties – for the synthesis of new polymers with different properties by post-polymerization modifications.

AUTHOR INFORMATION

Corresponding Author

S. Fadlallah, E-mail: sami.fadlallah@agroparistech.fr

F. Allais, E-mail: florent.allais@agroparistech.fr

Notes

There are no conflicts to declare

ACKNOWLEDGMENT

The authors are grateful to Grand Reims, Département de la Marne and Grand Est for financial support.

REFERENCES

[1] M.A. Gauthier, M.I. Gibson, H.-A. Klok, Synthesis of Functional Polymers by Post-Polymerization Modification, Angew. Chem. Int. Ed. 48 (2009) 48–58. https://doi.org/10.1002/anie.200801951.

[2] J. Seppälä, B. van Bochove, A. Lendlein, Developing Advanced Functional Polymers for Biomedical Applications, Biomacromolecules. 21 (2020) 273–275. https://doi.org/10.1021/acs.biomac.9b01701.

[3] W. Chen, H. Yang, R. Wang, R. Cheng, F. Meng, W. Wei, Z. Zhong, Versatile Synthesis of Functional Biodegradable Polymers by Combining Ring-Opening Polymerization and Postpolymerization Modification via Michael-Type Addition Reaction, Macromolecules. 43 (2010) 201–207. https://doi.org/10.1021/ma901897y.

[4] E.V. Pronina, Y.A. Vorotnikov, T.N. Pozmogova, A.O. Solovieva, S.M. Miroshnichenko, P.E. Plyusnin, D.P. Pishchur, I.V. Eltsov, M.V. Edeleva, M.A. Shestopalov, O.A. Efremova, No Catalyst Added Hydrogen Peroxide Oxidation of Dextran: An Environmentally Friendly Route to Multifunctional Polymers, ACS Sustain. Chem. Eng. (2020). https://doi.org/10.1021/acssuschemeng.0c01030.

[5] Z. Cheng, X. Zhu, G.D. Fu, E.T. Kang, K.G. Neoh, Dual-Brush-Type Amphiphilic Triblock Copolymer with Intact Epoxide Functional Groups from Consecutive RAFT Polymerizations and ATRP, Macromolecules. 38 (2005) 7187–7192. https://doi.org/10.1021/ma050536a.

[6] G.G. Odian, Principles of polymerization, 3rd ed, Wiley, New York, 1991.

[7] C. Mangold, F. Wurm, H. Frey, Functional PEG-based polymers with reactive groups via anionic ROP of tailor-made epoxides, Polym. Chem. 3 (2012) 1714. https://doi.org/10.1039/c2py00489e.

[8] S. Sugihara, A. Yoshida, S. Fujita, Y. Maeda, Design of Hydroxy-Functionalized Thermoresponsive Copolymers: Improved Direct Radical Polymerization of Hydroxy-Functional Vinyl Ethers, Macromolecules. 50 (2017) 8346–8356. https://doi.org/10.1021/acs.macromol.7b02084.

[9] S. Sutthasupa, M. Shiotsuki, F. Sanda, Recent advances in ring-opening metathesis polymerization, and application to synthesis of functional materials, Polym. J. 42 (2010) 905–915. https://doi.org/10.1038/pj.2010.94.
[10] M.M. Flook, V.W.L. Ng, R.R. Schrock, Synthesis of *cis,syndiotactic* ROMP Polymers Containing Alternating Enantiomers, J. Am. Chem. Soc. 133 (2011) 1784–1786. https://doi.org/10.1021/ja110949f.
[11] L.E. Rosebrugh, V.M. Marx, B.K. Keitz, R.H. Grubbs, Synthesis of Highly Cis, Syndiotactic Polymers via Ring-Opening Metathesis Polymerization Using Ruthenium Metathesis Catalysts, J. Am. Chem. Soc. 135 (2013) 10032–10035. https://doi.org/10.1021/ja405559y.
[12] M.A. Hillmyer, S.T. Nguyen, R.H. Grubbs, Utility of a Ruthenium Metathesis Catalyst for the Preparation of End-Functionalized Polybutadiene, Macromolecules. 30 (1997) 718–721. https://doi.org/10.1021/ma961316n.
[13] T. Morita, B.R. Maughon, C.W. Bielawski, R.H. Grubbs, A Ring-Opening Metathesis Polymerization (ROMP) Approach to Carboxyl- and Amino-Terminated Telechelic Poly(butadiene)s, Macromolecules. 33 (2000) 6621–6623. https://doi.org/10.1021/ma000013x.
[14] C.W. Bielawski, D. Benitez, T. Morita, R.H. Grubbs, Synthesis of End-Functionalized Poly(norbornene)s via Ring-Opening Metathesis Polymerization, Macromolecules. 34 (2001) 8610–8618. https://doi.org/10.1021/ma010878q.
[15] J.T. Patton, J.M. Boncella, K.B. Wagener, Acyclic diene metathesis (ADMET) polymerization: the synthesis of unsaturated polyesters, Macromolecules. 25 (1992) 3862–3867. https://doi.org/10.1021/ma00041a006.
[16] W. Gao, R. Hagver, V. Shah, W. Xie, R.A. Gross, M.F. Ilker, C. Bell, K.A. Burke, E.B. Coughlin, Glycolipid Polymer Synthesized from Natural Lactonic Sophorolipids by Ring-Opening Metathesis Polymerization, Macromolecules. 40 (2007) 145–147. https://doi.org/10.1021/ma0620159.
[17] H. Mutlu, M.A.R. Meier, Ring-opening metathesis polymerization of fatty acid derived monomers, J. Polym. Sci. Part Polym. Chem. 48 (2010) 5899–5906. https://doi.org/10.1002/pola.24401.
[18] E. Grau, S. Mecking, Polyterpenes by ring opening metathesis polymerization of caryophyllene and humulene, Green Chem. 15 (2013) 1112–1115. https://doi.org/10.1039/C3GC40300A.
[19] Z.J. Witczak, Levoglucosenone: A Versatile Carbohydrate Precursor for the Synthesis of Natural Products, in: Stud. Nat. Prod. Chem., Elsevier, 1994: pp. 267–281. https://doi.org/10.1016/B978-0-444-81780-8.50012-0.
[20] X. Ma, X. Liu, P. Yates, W. Raverty, M.G. Banwell, C. Ma, A.C. Willis, P.D. Carr, Manipulating the enone moiety of levoglucosenone: 1,3-Transposition reactions including ones leading to isolevoglucosenone, Tetrahedron. 74 (2018) 5000–5011. https://doi.org/10.1016/j.tet.2018.03.023.
[21] G.R. Court, C.H. Lawrence, W.D. Raverty, A.J. Duncan, Method for converting lignocellulosic materials into useful chemicals, US20120111714A1, 2012. https://patents.google.com/patent/US20120111714A1/en (accessed April 2, 2020).
[22] T. Debsharma, F.N. Behrendt, A. Laschewsky, H. Schlaad, Ring-Opening Metathesis Polymerization of Biomass-Derived Levoglucosenol, Angew. Chem. 131 (2019) 6790–6793. https://doi.org/10.1002/ange.201814501.

[23] T. Debsharma, Y. Yagci, H. Schlaad, Cellulose-Derived Functional Polyacetal by Cationic Ring-Opening Polymerization of Levoglucosenyl Methyl Ether, Angew. Chem. Int. Ed. 58 (2019) 18492–18495. https://doi.org/10.1002/anie.201908458.
[24] D.D. Ward, F. Shafizadeh, Cycloaddition "4 + 2" reactions of levoglucosenone, Carbohydr. Res. 95 (1981) 155–176. https://doi.org/10.1016/S0008-6215(00)85573-1.
[25] P. Bhaté, D. Horton, Stereoselective synthesis of functionalized carbocycles by cycloaddition to levoglucosenone, Carbohydr. Res. 122 (1983) 189–199. https://doi.org/10.1016/0008-6215(83)88330-X.
[26] F. Shafizadeh, M.G. Essrc, D.D. Ward, Additional reactions of levoglucosenone, Carbohydr. Res. 114 (1983) 71–82. https://doi.org/10.1016/0008-6215(83)88174-9
[27] Yu.A. Khalilova, O.Yu. Doronina, B.T. Sharipov, L.V. Spirikhin, F.A. Valeev, Eleuthesides and their analogs: III. Reaction of Red-Al with γ,δ-epoxy nitriles, Russ. J. Org. Chem. 49 (2013) 986–994. https://doi.org/10.1134/S1070428013070051.
[28] A.N. Davydova, A.A. Pershin, B.T. Sharipov, F.A. Valeev, Synthesis of chiral 2,3-cis-fused butan-4-olides from levoglucosenone–1,3-diene Diels–Alder adducts, Mendeleev Commun. 25 (2015) 271–272. https://doi.org/10.1016/j.mencom.2015.07.013.
[29] A.R. Tagirov, I.M. Biktagirov, Yu.S. Galimova, L.Kh. Faizullina, Sh.M. Salikhov, F.A. Valeev, Opening of the 1,6-anhydro bridge with selective reduction of the acetal moiety in levoglucosenone and its derivatives, Russ. J. Org. Chem. 51 (2015) 569–575. https://doi.org/10.1134/S1070428015040181.
[30] A.L. Flourat, A. Haudrechy, F. Allais, J.-H. Renault, (*S*)-γ-Hydroxymethyl-α,β-butenolide, a Valuable Chiral Synthon: Syntheses, Reactivity, and Applications, Org. Process Res. Dev. (2020) acs.oprd.9b00468. https://doi.org/10.1021/acs.oprd.9b00468.
[31] A.A.M. Peru, A.L. Flourat, C. Gunawan, W. Raverty, M. Jevric, B.W. Greatrex, F. Allais, Chemo-Enzymatic Synthesis of Chiral Epoxides Ethyl and Methyl (S)-3-(Oxiran-2-yl)propanoates from Renewable Levoglucosenone: An Access to Enantiopure (S)-Dairy Lactone, Molecules. 21 (2016) 988. https://doi.org/10.3390/molecules21080988.
[32] M.G. Banwell, X. Liu, L.A. Connal, M.G. Gardiner, Synthesis of Functionally and Stereochemically Diverse Polymers via Ring-Opening Metathesis Polymerization of Derivatives of the Biomass-Derived Platform Molecule Levoglucosenone Produced at Industrial Scale, Macromolecules. (2020). https://doi.org/10.1021/acs.macromol.0c01305.
[33] J. Krupka, Kinetics of thermal dimerization of cyclopentadiene and methylcyclopentadienes and their codimerization, Pet. Coal. 52 (2010) 290–306.
[34] G. Bonneau, A.A.M. Peru, A.L. Flourat, F. Allais, Organic solvent- and catalyst-free Baeyer–Villiger oxidation of levoglucosenone and dihydrolevoglucosenone (Cyrene®): a sustainable route to (S)-γ-hydroxymethyl-α,β-butenolide and (S)-γ-hydroxymethyl-γ-butyrolactone, Green Chem. 20 (2018) 2455–2458. https://doi.org/10.1039/C8GC00553B.
[35] M. Scholl, S. Ding, C.W. Lee, R.H. Grubbs, Synthesis and Activity of a New Generation of Ruthenium-Based Olefin Metathesis Catalysts Coordinated with 1,3-Dimesityl-4,5-dihydroimidazol-2-ylidene Ligands, Org. Lett. 1 (1999) 953–956. https://doi.org/10.1021/ol990909q.
[36] P. Schwab, M.B. France, J.W. Ziller, R.H. Grubbs, A Series of Well-Defined Metathesis Catalysts–Synthesis of [$RuCl_2(CHR')(PR_3)_2$] and Its Reactions, Angew. Chem. Int. Ed. Engl. 34 (1995) 2039–2041. https://doi.org/10.1002/anie.199520391.
[37] C.W. Bielawski, R.H. Grubbs, Living ring-opening metathesis polymerization, Prog. Polym. Sci. 32 (2007) 1–29. https://doi.org/10.1016/j.progpolymsci.2006.08.006.

[38] R.A. Sheldon, The E factor 25 years on: the rise of green chemistry and sustainability, Green Chem. 19 (2017) 18–43. https://doi.org/10.1039/C6GC02157C.
[39] J.D. Rule, J.S. Moore, ROMP Reactivity of endo- and exo-Dicyclopentadiene, Macromolecules. 35 (2002) 7878–7882. https://doi.org/10.1021/ma0209489.
[40] P.M. Molton, T.F. Demmitt, Reaction mechanisms in cellulose pyrolysis: a literature review, Battelle Pacific Northwest Labs., Richland, WA (USA), 1977. https://doi.org/10.2172/7298596.
[41] F. Diot-Néant, E. Rastoder, S.A. Miller, F. Allais, Chemo-Enzymatic Synthesis and Free Radical Polymerization of Renewable Acrylate Monomers from Cellulose-Based Lactones, ACS Sustain. Chem. Eng. 6 (2018) 17284–17293. https://doi.org/10.1021/acssuschemeng.8b04707.
[42] F. Diot-Néant, L. Mouterde, S. Fadlallah, S.A. Miller, F. Allais, Sustainable synthesis and polycondensation of Levoglucosenone-Cyrene™-based bicyclic diol monomer: an access to renewable polyesters, ChemSusChem. (2020). https://doi.org/10.1002/cssc.202000680.
[43] P. Ray, T. Hughes, C. Smith, G.P. Simon, K. Saito, Synthesis of Bioacrylic Polymers from Dihydro-5-hydroxyl furan-2-one (2H-HBO) by Free and Controlled Radical Polymerization, ACS Omega. 3 (2018) 2040–2048. https://doi.org/10.1021/acsomega.7b01929.
[44] P. Ray, T. Hughes, C. Smith, M. Hibbert, K. Saito, G.P. Simon, Development of bio-acrylic polymers from Cyrene™: transforming a green solvent to a green polymer, Polym. Chem. 10 (2019) 3334–3341. https://doi.org/10.1039/C9PY00353C.

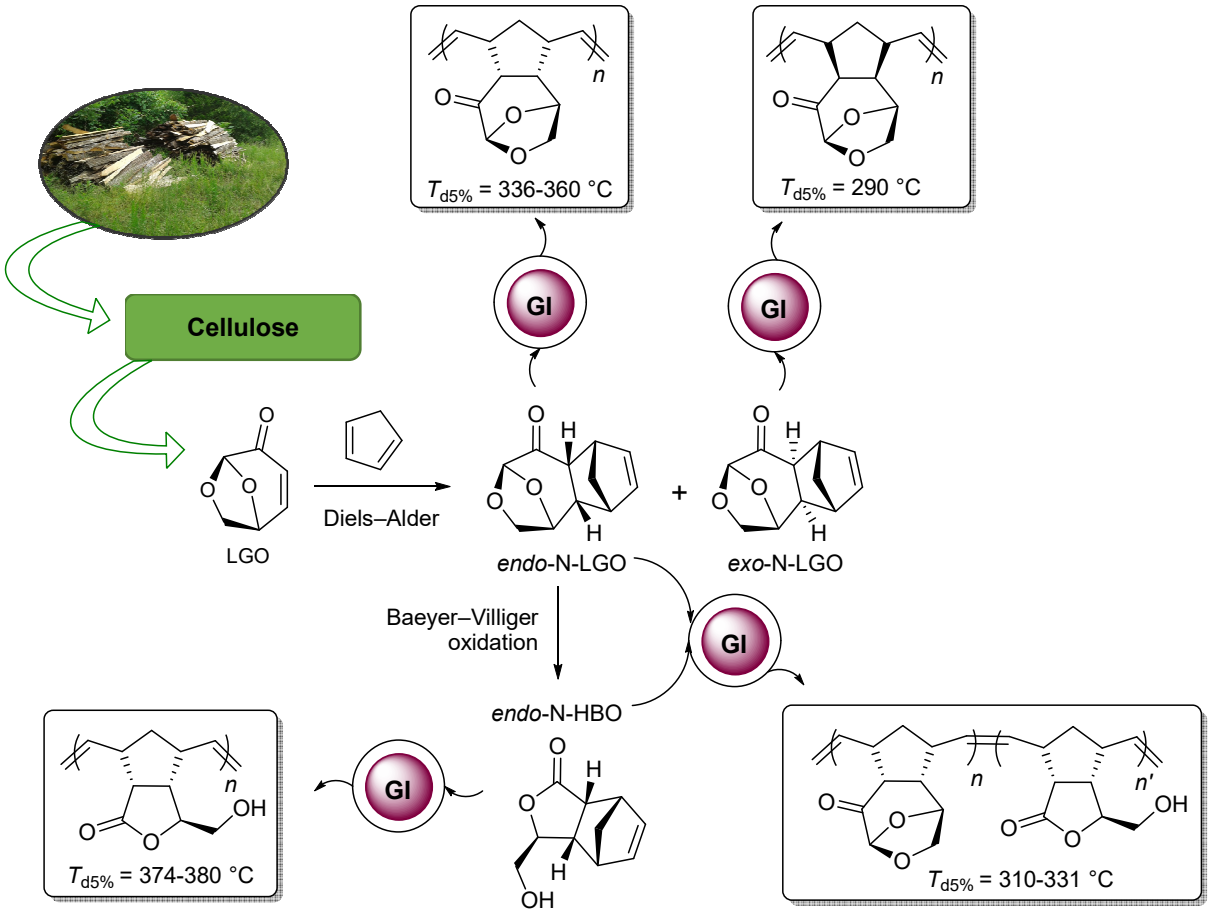

SYNOPSIS

Ring Opening Metathesis Polymerization (ROMP) of norbornene-based monomers synthesized from cellulose-derived LGO provide functional polymers that can compete with current fossil-fuel-based commodity polymers.

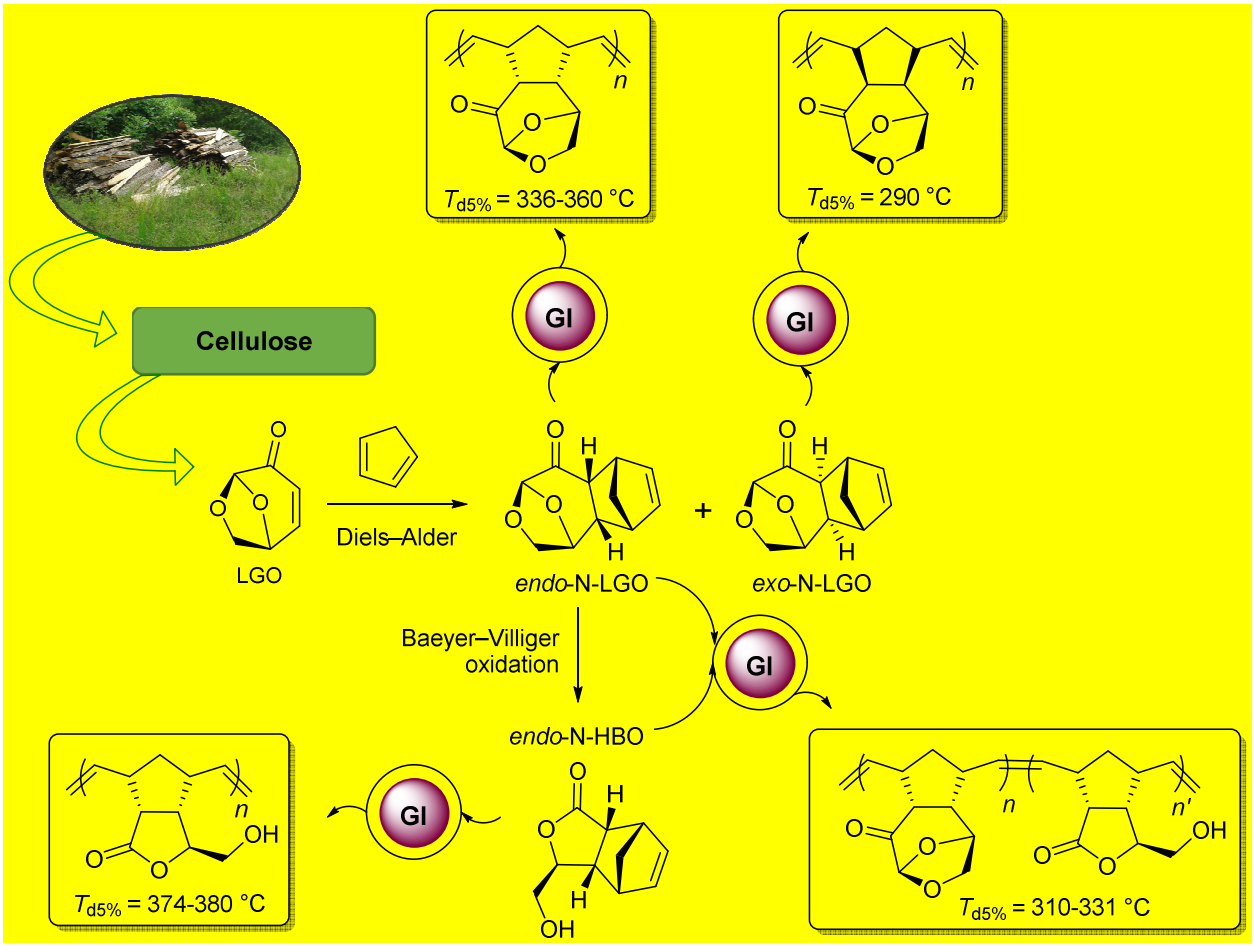
Cellulose
LGO
Diels–Alder
endo-N-LGO
exo-N-LGO
GI
GI
GI
Baeyer–Villiger oxidation
endo-N-HBO
GI
$T_{d5\%}$ = 336-360 °C
$T_{d5\%}$ = 290 °C
$T_{d5\%}$ = 374-380 °C
$T_{d5\%}$ = 310-331 °C